metals

MDPI

Article

Corrosion of Fe-(9~37) wt. %Cr Alloys at 700–800 °C in (N_2, H_2O, H_2S)-Mixed Gas

Min Jung Kim, Muhammad Ali Abro and Dong Bok Lee *

School of Advanced Materials Science and Engineering, Sungkyunkwan University, Suwon 16419, Korea; abc1219@skku.edu (M.J.K.); abromdali@gmail.com (M.A.A.)

* Correspondence: dlee@skku.ac.kr; Tel.: +82-31-290-7371

Academic Editor: Robert Tuttle

Received: 18 October 2016; Accepted: 15 November 2016; Published: 23 November 2016

Abstract: Fe-(9, 19, 28, 37) wt. %Cr alloys were corroded at 700 and 800 °C for 70 h under 1 atm of N_2, 1 atm of N_2/3.2%H_2O mixed gas, and 1 atm of N_2/3.1%H_2O/2.42%H_2S mixed gas. In this gas composition order, the corrosion rate of Fe-9Cr alloy rapidly increased. Fe-9Cr alloy was always non-protective. In contrast, Fe-(19, 28, 37) wt. %Cr alloys were protective in N_2 and N_2/3.2%H_2O mixed gas because of the formation of the Cr_2O_3 layer. They, however, became nonprotective in N_2/3.1%H_2O/2.42%H_2S mixed gas because sulfidation dominated to form the outer FeS layer and the inner Cr_2S_3 layer containing some $FeCr_2S_4$.

Keywords: Fe-Cr alloy; oxidation; sulfidation; H_2S corrosion

1. Introduction

Fe-Cr alloys are widely used as high-temperature structural materials. They oxidize when exposed to air or oxygen at high temperatures. When the Cr content in iron was ~5 wt. %, triple oxide layers such as Fe_2O_3/Fe_3O_4/FeO formed, and the oxidation rate was mainly controlled by the growth rate of FeO that formed on the alloy side [1]. The non-stoichiometric wustite grows much faster than the nearly stoichiometric Fe_3O_4 and Fe_2O_3. With an increase in the Cr content to ~10 wt. %, dispersed particles of the $FeCr_2O_4$ spinel formed more inside the FeO layer, and $FeCr_2O_4$ particles blocked the diffusion of Fe^{2+} ions to make the FeO layer thinner. With the further increase in the Cr content to ~15 wt. %, a mixed spinel, $Fe(Fe,Cr)_2O_4$, formed, which decreased the oxidation rate significantly. When the Cr content exceeded ~20 wt. %, the oxidation rate dropped sharply, forming a thin, continuous Cr_2O_3 layer containing a small amount of dissolved Fe ions [1–3]. When Fe-Cr alloys were exposed to S_2 gas at 1 atm, an FeS layer formed below 1.86 wt. %Cr, an outer $Fe_{1-x}S$ layer and an inner (FeS, $FeCr_2S_4$) mixed layer formed in the range of 1.86–38.3 wt. %Cr, and a solid solution of FeS-Cr_2S_3 formed above 38.3 wt. %Cr [4]. Although Cr decreased the sulfidation rate, even Fe-Cr alloys with high Cr contents displayed insufficient corrosion resistance. This is attributed to the fact that sulfidation rates of common metals are 10–100 times faster than oxidation rates because the sulfides have much larger defect concentrations and lower melting points than the corresponding oxides [5]. The sulfidation of Fe-(20, 25, 30) wt. %Cr steels in 94Ar/5H_2/1H_2S mixed gas at 600 °C for 718 h resulted in the formation of the outer FeS layer and the inner $FeCr_2S_4$ layer [6]. On the other hand, the corrosion of conventional oxidation-resistant alloys by water vapor and H_2S gas has been a serious problem [3]. Water vapor and H_2S gas release hydrogen atoms, which ingress in the metals interstitially, form hydrogen clusters, and cause hydrogen embrittlement. Water vapor that is present in many industrial gases can form metal hydrides, and change not only the reaction at the scale/metal interface but also the mass transfer in scales, accelerating the corrosion rate [3,7]. In this study, Fe-Cr alloys were corroded at 700 and 800 °C in (N_2, H_2O, H_2S) mixed gas in order to understand their corrosion behavior in hostile (H_2O, H_2S)-containing environments for practical applications. The aim

of this study is to examine the influence of the Cr content and the (N_2, H_2O, H_2S)-containing gas on the high-temperature corrosion of Fe-Cr alloys, which has not been adequately investigated before.

2. Experimental Procedures

Four kinds of hot-rolled ferritic Fe-Cr alloy sheets, viz., Fe-(8.5, 18.5, 28.3, 36.9) wt. %Cr, were prepared. They are termed as Fe-(9, 19, 28, 37)Cr, respectively, in this study. They were homogenized at 900 °C for 1 h under vacuum, cut into a size of 2 mm × 10 mm × 15 mm, ground up to a 1000-grit finish with SiC papers, ultrasonically cleaned in acetone, and corroded at 700 and 800 °C for 70 h under 1 atm of total pressure. Each test coupon was suspended by a Pt wire in a quartz reaction tube within the hot zone of an electrical furnace (Ajeon, Seoul, Korea), as shown in Figure 1. Three kinds of corrosion atmospheres were employed, viz. 1 atm of N_2, (0.968 atm of N_2 plus 0.032 atm of H_2O) that was achieved by bubbling the N_2 gas through the water bath kept at 25 °C, and (0.9448 atm of N_2 plus 0.031 atm of H_2O plus 0.0242 atm of H_2S) that was achieved by bubbling N_2 gas through the water bath kept at 25 °C and simultaneously flowing the N_2-5%H_2S gas into the quartz reaction tube. The N_2 gas was 99.999% pure, and H_2S gas was 99.5% pure. Nitrogen gas was blown into the reaction tube during heating and cooling stages. After finishing the corrosion test in N_2, N_2/3.2%H_2O, and N_2/3.1%H_2O/2.42%H_2S gas, the test coupons were furnace-cooled, and characterized by a scanning electron microscope (SEM, Jeol JSM-6390A, Tokyo, Japan), a high-power X-ray diffractometer (XRD, Mac Science M18XHF-SRA, Yokohama, Japan) with Cu-Kα radiation operating at 40 kV and 300 mA, and an electron probe microanalyzer (EPMA, Shimadzu, EPMA 1600, Kyoto, Japan).

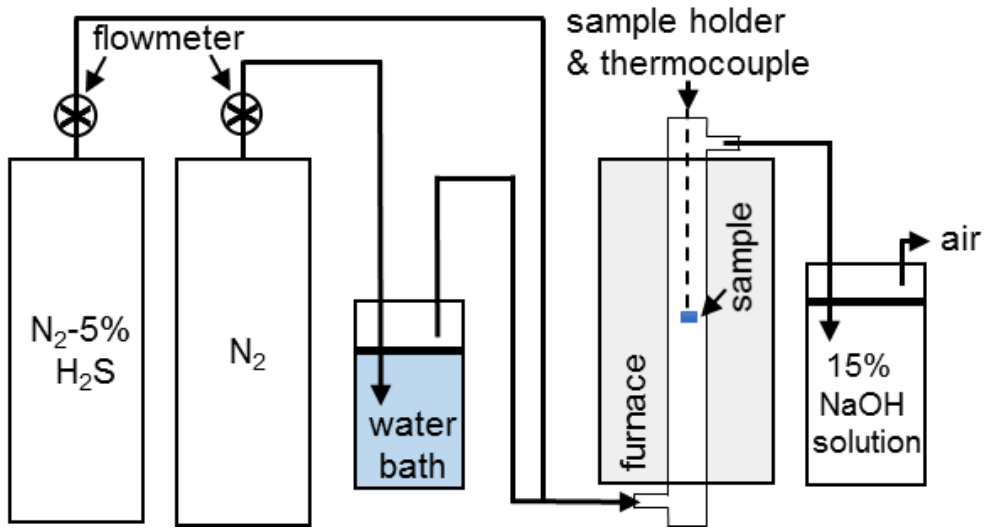

Figure 1. Corrosion testing apparatus.

3. Results and Discussion

Table 1 lists the weight gains of Fe-(9, 19, 28, 37)Cr alloys due to corrosion at 700 and 800 °C for 70 h, which were measured using a microbalance before and after corrosion. Fe-9Cr always displayed the worst corrosion resistance, gaining excessive weight. For example, Fe-9Cr oxidized fast even in the N_2 gas through the reaction with impurities such as 3 ppm H_2O and 2 ppm O_2 in the N_2 gas (99.999% pure). Fe-9Cr oxidized faster in the N_2/H_2O gas than in the N_2 gas because of water vapor [7]. Water vapor dissociates into oxygen and hydrogen, oxidizes the metal, and forms voids within the oxide scale according to the equation [1,3],

$$M + H_2O \rightarrow MO + (2H \text{ or } H_2) \quad (1)$$

Table 1. Weight gain of Fe-(9, 19, 28, 37)Cr alloys measured after corrosion at 700 and 800 °C for 70 h under 1 atm of N_2, $N_2/3.2\%H_2O$, and $N_2/3.1\%H_2O/2.42\%H_2S$ gas.

Temp.	Gas	Weight Gain (mg/cm^2)			
		9Cr	19Cr	28Cr	37Cr
700 °C	N_2	195	1–2	1–2	1–2
	N_2/H_2O	220	1–2	1–2	1–2
	$N_2/H_2O/H_2S$	2050	470	200	70
800 °C	N_2	235	1–2	1–2	1–2
	N_2/H_2O	400	1–2	1–2	1–2
	$N_2/H_2O/H_2S$	massive spalling	1530	690	550

Fe-9Cr corroded the most seriously in $N_2/H_2O/H_2S$ gas, because H_2S was much more harmful than H_2O. H_2S dissociates into hydrogen and sulfur. Sulfur forms non-protective metal sulfides according to the following equation:

$$M + H_2S \rightarrow MS + (2H \text{ or } H_2) \quad (2)$$

Hydrogen, which is released from H_2S and H_2O, dissolves and ingresses into the alloy and the scale interstitially, generates lattice point defects, forms hydrogen clusters and voids, causes hydrogen embrittlement, produces volatile hydrated species, and accelerates cracking, spallation and fracture of the scale. Hence, no metals are resistant to H_2O/H_2S corrosion. As listed in Table 1, Fe-(19, 29, 37)Cr displayed much better corrosion resistance in N_2 and $N_2/3.2\%H_2O$ with weight gains of 1–2 mg/cm^2 than Fe-9Cr. Fe-(19, 29, 37)Cr formed 0.3- to 1.3-μm-thick, adherent oxide scales. However, even Fe-(19, 29, 37)Cr failed in $N_2/3.1\%H_2O/2.42\%H_2S$ with large weight gains, forming non-adherent, fragile sulfide scales as thick as 35–750 μm. This scale failure made the weight gains measured in $N_2/H_2O/H_2S$ gas inaccurate. In $N_2/H_2O/H_2S$ gas, the amount of local cracking, spallation and void formation in the scale varied for each test run. Although the accurate measurement of weight gains in $N_2/H_2O/H_2S$ gas was impossible, it was clear that weight gains due to scaling decreased sharply with the addition of Cr.

Figure 2 shows the XRD patterns of scales formed after corrosion at 800 °C for 70 h. The corrosion of Fe-9Cr in N_2 and N_2/H_2O resulted in the formation of Fe_2O_3 and Fe_3O_4, as shown in Figure 2a,b. Oxide scales formed on Fe-9Cr in N_2 and N_2/H_2O were 90 and 100 μm thick, respectively. Since X-rays could not penetrate such thick oxide scales, FeO and Cr-oxides such as $FeCr_2O_4$, which might form next to the alloy [1], were absent in Figure 2a,b. In contrast, Fe-(19, 28, 37)Cr alloys oxidized at much slower rates in N_2 and N_2/H_2O than Fe-9Cr alloy, as listed in Table 1. Fe-(19, 28, 37)Cr alloys formed the protective Cr_2O_3 scale, as typically shown in Figure 2c,d. Here, the Fe-Cr peaks were strong owing to the thinness of the oxide scales. In Fe-(19, 28, 37)Cr alloys, Cr was dissolved in the α-Fe matrix.

Figure 3 shows the EPMA analytical results on the scales formed on Fe-9Cr after corrosion at 700 °C for 70 h. The oxide scales that formed after corrosion in N_2 and N_2/H_2O were about 90 and 140 μm thick, respectively. The scale morphology and elemental distribution in N_2 gas were similar to those in N_2/H_2O gas, as shown in Figure 3, indicating that the same oxidation mechanism operated in N_2 and N_2/H_2O gas. Voids were sporadically scattered in both oxide scales, below which the oxygen-affected zone (OAZ) existed. Voids formed owing to the volume expansion during scaling, hydrogen released from the water vapor, and the Kirkendall effect arose due to the outward diffusion of cations during scaling. In both oxide scales, the outer layer consisted of iron oxides, while the inner layer consisted of (Fe,Cr) mixed oxides. This indicated that Fe^{2+} and Fe^{3+} ions were more mobile than Cr^{3+} ions. The oxidation in N_2 and N_2/H_2O gas was mainly controlled by the outward diffusion of iron ions through the inner (Fe,Cr) mixed oxide layer. Iron oxidized preferentially in N_2 and N_2/H_2O gas because iron is the base element and its oxide, FeO, is a non-stoichiometric compound with a relatively fast growth rate.

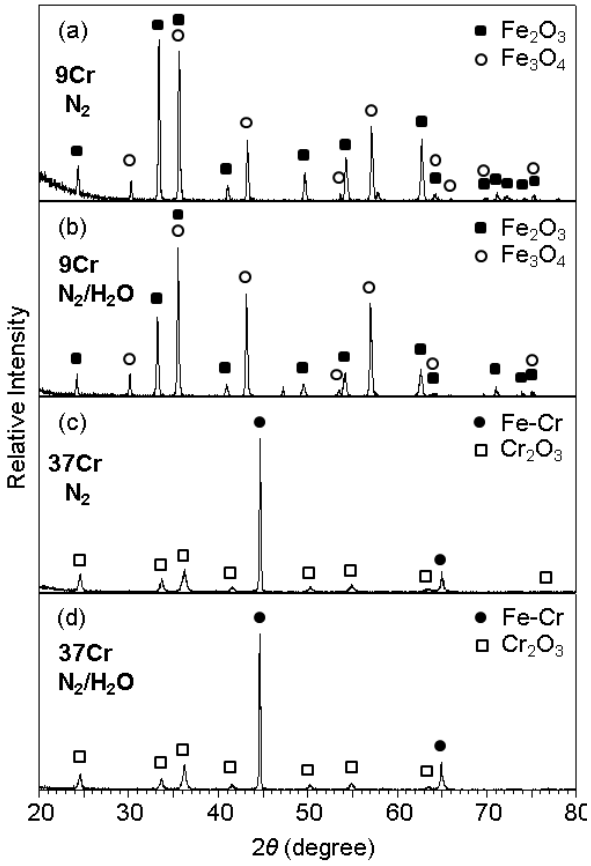

Figure 2. XRD patterns taken after corrosion testing at 800 °C for 70 h. (**a**) Fe-9Cr in N_2; (**b**) Fe-9Cr in N_2/3.2%H_2O; (**c**) Fe-37Cr in N_2; (**d**) Fe-37Cr in N_2/3.2%H_2O.

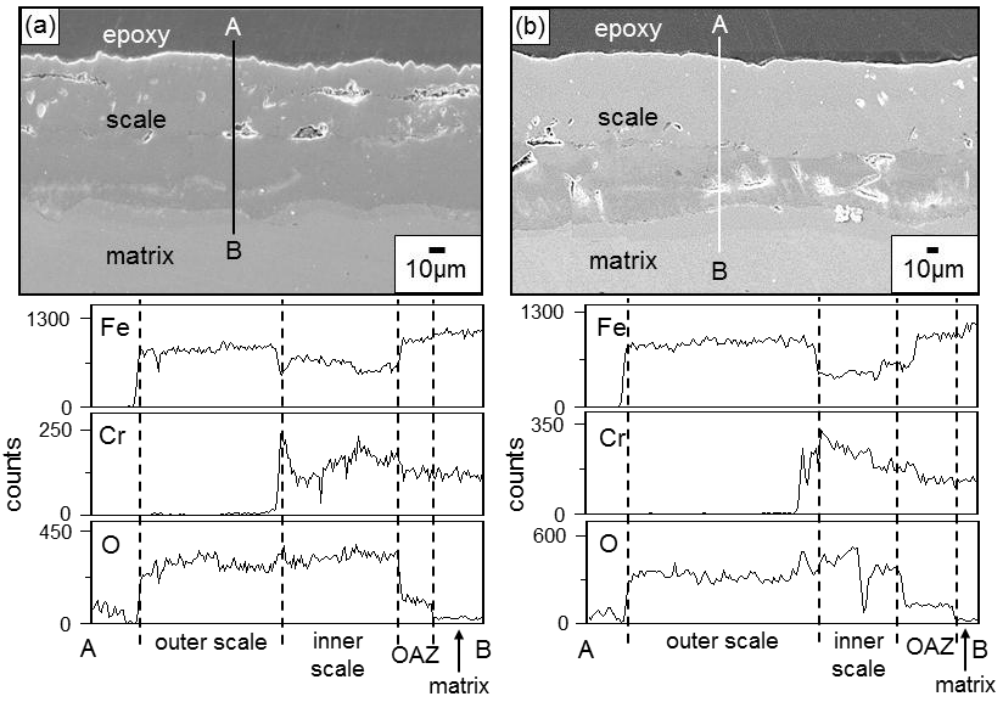

Figure 3. EPMA cross-section and line profiles of Fe-9Cr after corrosion at 700 °C for 70 h in (**a**) N_2; and (**b**) N_2/3.2%H_2O.

Figure 4 shows the EPMA analytical results on the scales formed on Fe-37Cr after corrosion at 700 °C for 70 h. The oxide scales that formed after corrosion in N_2 and N_2/H_2O were about 0.6 and 1.1 μm thick, respectively. In N_2 and N_2/H_2O gas, the Cr_2O_3 scale formed (Figure 2c,d), in which Fe was dissolved (Figure 4). The complete dissolution of Fe_2O_3 in Cr_2O_3 is possible, because Cr_2O_3 and Fe_2O_3 have the same rhombohedral structure [8]. Like Fe-37Cr, Fe-(19, 28)Cr also formed a thin Cr_2O_3 scale containing some Fe when they corroded in N_2 and N_2/H_2O gas. Once the thin but protective Cr_2O_3 scale formed, the outward diffusion of iron ions was suppressed so that good corrosion resistance was achieved.

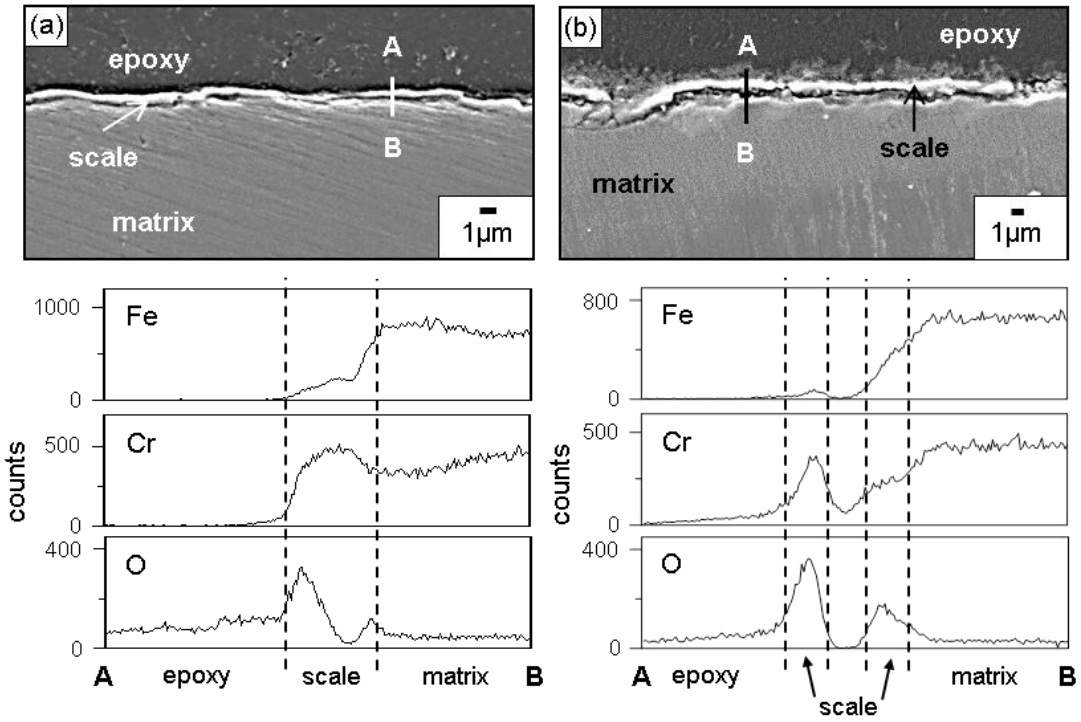

Figure 4. EPMA cross-section and line profiles of Fe-37Cr after corrosion at 700 °C for 70 h in (**a**) N_2; and (**b**) $N_2/3.2\%H_2O$.

In $N_2/3.1\%H_2O/2.42\%H_2S$ gas, Fe-(9-37)Cr alloys could not form Cr_2O_3, and corroded fast, as typically shown in Figure 5. The scales formed on Fe-(9, 19, 28, 37)Cr alloys consisted primarily of the outer FeS layer (Figure 5a), and the inner Cr_2S_3 layer containing some $FeCr_2S_4$ (Figure 5b). Since FeS grows fast owing to its high non-stoichiometry, outer FeS grains were coarser than the inner (Cr_2S_3, $FeCr_2S_4$) mixed grains. In Figure 5c, cracks propagated inter- and trans-granularly due mainly to the excessive growth stress generated in the thick outer scale. The scale shown in Figure 5d was about 100 μm thick, and had cracks and voids. A small amount of Cr was dissolved in the outer FeS layer (Figure 5e). The preferential sulfidation of iron in the outer FeS layer decreased the sulfur potential underneath, and thereby increased the oxygen potential in the inner Cr_2S_3-rich layer, leading to the incorporation of oxygen in the inner Cr_2S_3-rich layer. FeS is a p-type metal-deficit compound, which grows fast by the outward diffusion of Fe^{2+} ions [5,9,10]. Its defect chemical equation is as follows.

$$1/2O_2 = O_o + 2h^{\cdot} + V''_{Fe} \quad (3)$$

here, O_O, $h^{\cdot}$ and V''_{Fe} mean the O atom on the O site, the electron hole in the valence band with a + 1 charge, and the iron vacancy with a − 2 charge. The defect chemical reaction for the dissolution of Cr_2S_3 in FeS is as follows.

$$Cr_2S_3 = 2Cr^{\cdot}_{Fe} + V''_{Fe} + 3S_S \quad (4)$$

Hence, the doping of Cr^{3+} ions would increase the concentration of iron vacancies, leading to the enhancement of the FeS growth. Oxygen was incorporated in the inner Cr_2S_3-rich layer (Figure 5e). However, no oxides were detected in Figure 5b, because their amount was small or oxygen was dissolved in the sulfide scales. Grains in the inner layer were fine owing to the nucleation and growth of Cr_2S_3, together with some $FeCr_2S_4$ and probably some oxides. In $N_2/3.1\%H_2O/2.42\%H_2S$ gas, Fe-(9, 19, 28, 37)Cr alloys sulfidized preferentially owing to the high sulfur potential in the test gas.

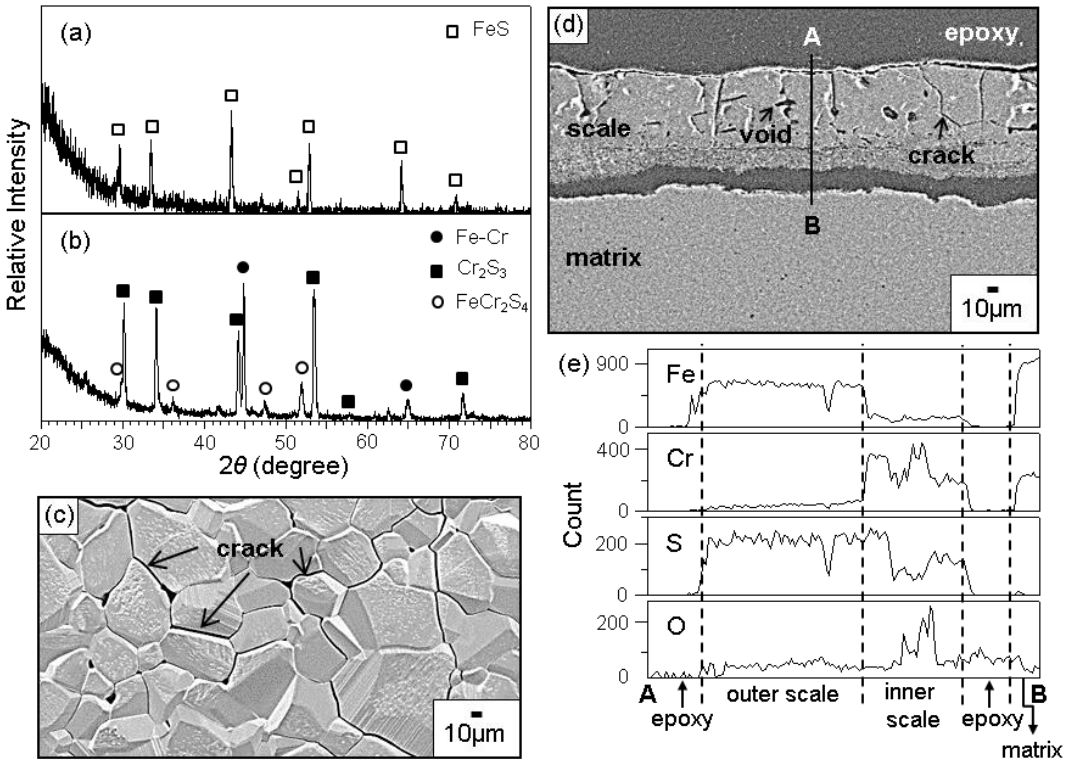

Figure 5. Fe-19Cr after corrosion at 700 °C for 40 h in $N_2/3.1\%H_2O/2.42\%H_2S$. (**a**) XRD pattern after corrosion; (**b**) XRD pattern taken after grinding off the outer scale; (**c**) SEM top view; (**d**) EPMA cross-section; (**e**) EPMA line profiles of along A–B denoted in (**d**).

4. Conclusions

When Fe-9Cr alloy corroded at 700 and 800 °C in N_2 and $N_2/3.2\%H_2O$ gas, thick, porous oxide scales formed, which consisted of the outer iron oxide layer and the inner (Fe,Cr) mixed oxide layer. Under the same corrosion condition, Fe-(19, 28, 37)Cr alloys formed thin, dense, protective Cr_2O_3 oxide layers, in which iron was dissolved to a certain extent. In $N_2/3.1\%H_2O/2.42\%H_2S$ gas, Fe-(9, 19, 28, 37)Cr alloys corroded fast, forming thick, non-adherent, fragile scales, which consisted of the outer FeS layer and the inner Cr_2S_3 layer containing some $FeCr_2S_4$. The preferential sulfidation of Fe-(9, 19, 28, 37)Cr alloys in the H_2S-containing gas was responsible for the poor corrosion resistance of Fe-(9, 19, 28, 37)Cr alloys.

Acknowledgments: This research was supported by Basic Science Research Program through the National Research Foundation of Korea (NRF) funded by the Ministry of Education (2016R1A2B1013169), Korea.

Author Contributions: Min Jung Kim conceived and designed the experimental procedure and drafted the paper. Muhammad Ali Abro prepared the samples, conducted the experiments and analyzed the data. All the results were discussed with Dong Bok Lee who supervised the experimental work and finalized the paper.

Conflicts of Interest: The authors declare no conflict of interest.

References

1. Birks, N.; Meier, G.H.; Pettit, F.S. *Introduction to High Temperature Oxidation of Metals*, 2nd ed.; Cambridge University: New York, NY, USA, 2006.
2. Khanna, A.S. *Introduction to High Temperature Oxidation and Corrosion*; ASM Int.: Metals Park, OH, USA, 2002; p. 135.
3. Young, D. *High Temperature Oxidation and Corrosion of Metals*; Elsevier: Oxford, UK, 2008.
4. Mrowec, S.; Walec, T.; Werber, T. High-temperature sulfur corrosion of iron-chromium alloys. *Oxid. Met.* **1969**, *1*, 93.
5. Mrowec, S.; Przybylski, K. Transport properties of sulfide scales and sulfidation of metals and alloys. *Oxid. Met.* **1985**, *23*, 107. [CrossRef]
6. Schulte, M.; Rahmel, A.; Schutze, M. The Sulfidation Behavior of Several Commercial Ferritic and Austenitic Steels. *Oxid. Met.* **1998**, *49*, 33. [CrossRef]
7. Saunders, S.R.J.; McCartney, L.N. Current Understanding of Steam Oxidation—Power Plant and Laboratory Experience. *Mater. Sci. Forum* **2006**, *119*, 522. [CrossRef]
8. Asteman, H.; Norling, R.; Svensson, J.-E.; Nylund, A.; Nyborg, L. Quantitative AES depth profiling of iron and chromium oxides in solid solution, $(Cr_{1-x}Fe_x)_2O_3$. *Surf. Interface Anal.* **2002**, *34*, 234. [CrossRef]
9. Mrowec, S.; Wedrychowska, M. Kinetics and mechanism of high-temperature sulfur corrosion of Fe-Cr-Al alloys. *Oxid. Met.* **1979**, *13*, 481. [CrossRef]
10. Danielewski, M.; Mrowec, S.; Stolosa, A. Sulfidation of iron at high temperatures and diffusion kinetics in ferrous sulfide. *Oxid. Met.* **1982**, *17*, 77. [CrossRef]

© 2016 by the authors; licensee MDPI, Basel, Switzerland. This article is an open access article distributed under the terms and conditions of the Creative Commons Attribution (CC-BY) license (http://creativecommons.org/licenses/by/4.0/).